Laser Beam Shaping with Computer-Generated Holograms for Fiducial Marking

A. Alkan Gulses[a], Shaildhish Rai[a], Joy Padiyar[a], Shannon Crowley[a], Alex Martin[a], Gabriel Islas[a], Russell M. Kurtz[a], Thomas Forrester[a], Daric Guimary[b]
[a]Luminit, LLC, 1850 W. 205th St., Torrance, CA 90501
[b]Defense Microelectronics Activity, 4234 54th St., McClellan, CA 95652

ABSTRACT

The laser marking method has obvious advantages over other available marking methods in speed, accuracy, and flexibility. Mask marking and beam deflection marking are typical methods, each having advantages and disadvantages. In the former, an opaque mask is directly imaged to create the desired mark. This method is practical and relatively fast, but most of the marking energy is blocked, losing efficiency. Additionally, this method requires a precise and bulky lens system. In the latter method, the focused beam is steered onto the sample, writing point by point. This technique has higher flexibility between marks, but it is slow, requires micro-movements, and accurate micro-motion parts are very expensive.

We propose an innovative, holographic approach in laser marking. In the new system, a holographic projection system based on a digitally designed computer-generated hologram (CGH) is employed. This specially designed, fully transparent, phase only CGH modulates the high-power writing beam to create any desired image in the far field, where the beam etches a permanent mark of that image onto the designated silicon wafer substrate. Holographic marking combines the advantages of mask and beam deflection marking methods, such as high speed and stationary operation with minimal power loss, in a relatively simple and inexpensive setup. Also, since the holographic projection maintains its image quality after a certain distance, the setup is less prone to spatial alignment errors. We believe that the proposed technique will make significant contributions in the field of laser marking.

Keywords: Fourier optics, diffractive optical elements, computer-generated holograms, CGH, beam shaping, laser machining, fiducial marking

1. INTRODUCTION

In 1947, the invention of the transistor birthed the electronics industry, followed by rapid developments starting in the second half of the 20th century. An indicator of this rapid development, which is commonly cited, is the so-called Moore's law, basically stating that the number of transistors per an integrated circuit doubles approximately every year. In conjunction with these developments, several other needs have emerged, one of which is the "labeling" of these manufactured electronic components. Among various labeling techniques, such as pen writing, press labeling, ink marking, chemical etching, and mechanical stamping, the laser marking method stands out, based on the fundamental criteria of speed, performance, and flexibility.

For the laser marking systems, current technology employs either mask marking or beam deflection marking methods. In the former, an opaque mask is directly imaged to create the desired mark. This method is practical, relatively fast, and more cost-effective than beam deflection. In the latter method, one must steer the focused beam onto the sample, and execute writing point by point. This technique has the advantage of possessing high flexibility between marks. However, both these techniques have certain disadvantages. For example, in the mask marking system, a significant portion of the incident light is blocked. This tends to require a higher-power laser, which is normally larger than beam deflection or the marking method described here. Not only will blocking the laser for shaping result in a loss of power, but the higher power requirement will also reduce the marking laser's lifetime. A larger laser component can reduce these effects but can also reduce the space available for other components. When it comes to the laser beam deflection scheme, the working platform will still be a problem due to demanding hardware for the high-resolution beam focusing and aiming. There are often micro-movements of the marking spot due to moving the laser between spots. In addition, writing even a single character can take several hours. These issues may prevent usage of beam-deflection marking in applications requiring serial processing. Furthermore, the cost of a beam deflection system is high.

Laser Beam Shaping XIX, edited by Angela Dudley and Alexander V. Laskin; August 12, 2019
Proc. of SPIE Vol. 11107, 11107-16 · © 2019 SPIE ·· doi: 10.1117/to come

On the other hand, holographic projection is an imaging technique that has several advantages over conventional imaging[1]. In this research, we examine fiducial marking of silicon wafers through computer-generated holograms (CGHs). The CGH, an almost completely transparent phase mask, is a diffractive optical element, essentially used to shape the laser beam into a fiducial mark, then project the desired mark onto the target in the far field. The CGH can modulate the beam instantaneously and without dissipating any extra power, redirecting the entire laser power into the marking area. Another advantage is accuracy; the system is more tolerant to spatial shifting than is classical imaging. Also, a holographic projection fiducial marking process does not require point-by-point operation, making it rapid, yielding much more precise results, and affording convenience and compact hardware. A few works in the literature describe the use of phase elements for laser marking. For example, in one work[2], researchers used 10-level phase elements to create point-wise drilling on silicon. Another study[3] included information on printing images on photographic paper by using a binary diffractive element.

In this research, we use a 256-level diffractive element to create sub-millimeter fiducial marks on silicon wafers. These images are very clean, especially considering the highly multimodal laser used for marking. We present a novel method of creating fine fiducial marking by using advanced holographic projection of a marking laser, passing through a computer-designed diffractive element. The design of the CGH is explained in Section 2, followed by experimental results in Section 3 and concluding remarks in Section 4.

As the importance of miniaturization increases rapidly in almost every area, we believe that the proposed technique and its results can make significant contributions not only in the specific field of laser marking but also in other relevant applications.

2. DESIGN OF THE CGHs FOR FIDUCIAL MARKING

2.1 Overview

Proposed by Dennis Gabor in 1948, holography enables recording of phase-fronts of electromagnetic waves, not just intensities as in photography[4]. Although holograms are traditionally recorded through experiments in an analog manner for real objects, it is also possible to record nonphysical objects, including 3D ones, by employing computer-generated holography[5].

Being a branch of digital holography, computer-generated holography is used to modulate wavefronts through diffraction, in a most general sense, to implement certain crucial functions, such as the 3D imaging of artificial (computer-designed) objects. Other usages of CGHs may be itemized as aspherical surface testing, optical interconnections, beam shaping, and optical image encryption. Beam shaping (energy redirection) is the most important of these for many applications.

Studies on CGHs date back to the 1960s, when they were called “synthetic holograms”[6]. The first CGHs were intensity patterns prepared by hand-drawing, and they would change both phase and amplitude on the same plane to reconstruct the desired pattern. These were not efficient since the opaque parts absorbed light, reducing throughput. Furthermore, each pixel of the desired pattern had to be represented by a window containing subpixels, resulting in a significant amount of space-bandwidth loss. In phase-only CGHs, however, only phase modulation is employed, although amplitude modulation can also be implemented with this phase function via utilization of phase-retrieval algorithms as well as stochastic (or heuristic) approaches. Also, since the element is completely transparent, no significant energy loss occurs. These phase-only transparent diffractive elements can be fabricated by semiconductor lithographic processing equipment, already developed to a very high technical level. With the appearance of advanced surface modulation techniques, as well as superior computation algorithms executed by computers, phase-only CGHs are being recognized as high-quality, cost-efficient solutions for the applications listed in the previous paragraph.

2.2 CGH Principles

A sample operation of an imaging CGH is illustrated in Figure 1. A surface relief structure (ideally, completely transmissive, and with appropriate coatings) with a certain quantization level (represented as Q to denote the number of phase levels) is the CGH element of interest. The structure works by selectively diffracting light through its digitally designed pixels. Thereby, it modulates the wavefronts of an illuminating source in a desired way. The information is computed first, and written on the unit CGH, followed by replication. In the figure, the CGH is a transparent phase plate at the plane $z = 0$. It has pixels with feature size δ and minimum depth β. The total device side length is T and one unit side length of the CGH is L. Note that in the figure, Q is illustrated as 4 and replication of the unit CGH is illustrated as 2×2. A Fourier transform lens (a lens that focuses a collimated input onto the image plane) is exploited for a better-quality

image. At the focal length, a screen exists at the (ξ, η) plane, with the traditional "Lena" image for illustration. The dispersion angle of the element is shown, with θ defining the field of view (FOV) of the system.

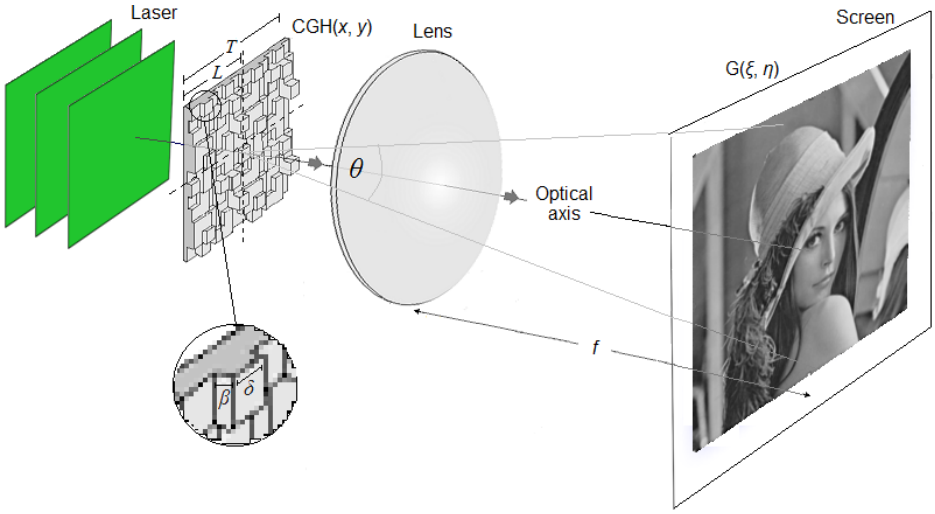

Figure 1. A standard CGH operation is illustrated to reconstruct a sample "Lena" image based on the holographic projection principle. The divergence angle, θ, defines the width of the projected image. f is the focal length of the lens. The parameter δ is the pixel size, β is the pixel depth (as shown by the enlarged section), and quantization and replication values are illustrated as 4 and 2 × 2, respectively.

A shown in Figure 1, the CGH diffracts the collimated coherent laser illumination to the image plane at the focus of the lens, so that the field at the (ξ, η) plane is the Fourier transform of that at the (x, y) plane. This far-field reconstruction pattern combines the input mode distribution with the CGH phase pattern. In this model, the laser illumination approximates a plane wave, so the field $G(\xi, \eta)$ on the screen is the Fourier transform of the field induced by the CGH phase pattern.

$$G(\xi,\eta) = C \iint \psi(x,y) CGH(x,y) exp\left[-i\frac{2\pi}{\lambda f}(\xi x + \eta y)\right] dx\, dy \tag{1a}$$

$$G(p,q) = C \sum_{m=-\frac{M}{2}}^{\frac{M}{2}-1} \sum_{n=-\frac{N}{2}}^{\frac{N}{2}-1} \psi(m,n) CGH(m,n)\, exp\left[-i2\pi\left(\frac{pm}{M} + \frac{qn}{N}\right)\right] \tag{1b}$$

Equation (1a) is the continuous form and Equation (1b) is the discrete form used in digital computations[7]. In these equations, C is a collection of constants of amplitude and phase that balances the integrated energy on both sides of the equal sign, λ is the illumination wavelength, and f is the focal length of the Fourier transform lens. For the discrete version, we employ a discrete coordinate system, shown as $x \rightarrow m$, $y \rightarrow n$ and $\xi \rightarrow p$, $\eta \rightarrow q$. M and N correspond to the total number of pixels in the x and y dimensions. At the image plane, the image pixel size (resolution) is $(\Delta p, \Delta q) = (\lambda f_p/T, \lambda f_q/T)$, and total image size is $(M\Delta p, N\Delta q) = (\lambda f_p/\delta, \lambda f_q/\delta)$.

In the operational sense, the above discussion means that for small angles of θ, the dispersion is $\sin(\theta) = \lambda/\delta$. This equation is useful in computing the desired performance. Also, the pixel depth, β, is important as a fabrication parameter, and as expected, it depends on the quantization, Q, and index difference Δn, indicating the difference of refractive indices between the material and the air. The minimum acceptable surface depth is $\beta = \lambda/(Q\Delta n)$[8].

2.3 Computation

Having defined the fundamental operation and related parameters of a CGH-type projective system in Section 2.2, we now discuss the overall design approach to compute the CGH diffractive surface maps. A pure phase function $CGH(x, y)$ whose Fourier transform gives the desired image needs to be found. An inverse transform of the desired pattern cannot be used directly, since the Fourier transform includes amplitude information that is lost on the CGH plane. Instead, advanced algorithms are used to compensate for the lack of amplitude information. That way, one can make high-performance CGHs with excellent image quality and good diffraction efficiency.

The design algorithms can be classified under deterministic or stochastic approaches[8]. The former includes algorithms like gradient search or iterative Fourier transform (also known as Gerchberg-Saxton) algorithms, and the latter contains a variety of heuristic approaches such as simulated annealing or a genetic algorithm. The iterative Fourier transform algorithm (IFTA) is convenient from the perspective of computation time, and is generally sufficiently accurate. In the application, one starts with a grid of random phases. The grid is propagated to the screen, as described by Equations (1). At the screen plane, the desired amplitude distribution is imposed while keeping the phases unchanged. Inverse propagation is executed with the same equations but with the complex conjugate of the integrand. At the device plane all intensity values are reset to one without affecting the phase. This process is repeated until the mean-squared error (MSE) stops decreasing and reaches its asymptote. The MSE can never be zero due to elimination of the amplitude in the CGH calculations. This creates noise that cannot be eliminated. Other sources of noise are fabrication defects, laser speckle, and laser spot size dimensions. The resultant pattern is multiplexed for speckle reduction and to cover the collimated laser area, reducing or eliminating the laser-related errors; fabrication and calculation limitations cannot be reduced so easily.

3. EXPERIMENTAL DEMONSTRATION OF FIDUCIAL MARKING

3.1 CGH Operation

A CGH designed using the iterative Fourier transform algorithm (IFTA) method requires coherent illumination to operate. We start with Equation (1) to see the result of the real operation of a CGH. Equation (1a), used for these designs, implements a Fourier transform. Representing the transform as "$\mathfrak{F}$", Equation (1a) can be rewritten by using the convolution theorem[9]. In Equation 2, $\otimes$ represents the convolution operation.

$$\mathfrak{F}\{\psi(x,y)CGH(x,y)\} = \mathfrak{F}\big(\psi(x,y)\big) \otimes \mathfrak{F}\big(CGH(x,y)\big) \tag{2}$$

When the CGH is multiplexed, Equation (2) can be expanded by inserting the CGH replication term, which is the Dirac comb function (a sequence of Dirac delta functions separated by the period L), and reapplying the convolution theorem.

$$\mathfrak{F}\{\psi(x,y)CGH(x,y)\} = \mathfrak{F}\{\psi(x,y)\} \otimes \mathfrak{F}\left\{CGH_{unit}(x,y) \otimes comb\left(\frac{x}{L},\frac{y}{L}\right)\right\} \tag{3a}$$

$$= \mathfrak{F}\{\psi(x,y)\} \otimes \left(\mathfrak{F}\{CGH_{unit}(x,y)\}comb\big(Lf_x, Lf_y\big)\right) \tag{3b}$$

In Equations (3), the middle term is the transform of the unit element that yields the desired image based on the result of the algorithm. This result is multiplied by a grid whose period is inversely proportional to L, defined by the rightmost comb function, and this set is further convolved with the transform of the modal pattern of the laser. Here f_x and f_y are the spatial frequencies dependent on the coordinates (ξ, η). In addition, in Equations (3), components come from the pixelated structure of the element and from the overall boundaries encircled by a square of feature size T. The former creates a "sinc" modulation that can be avoided during the design stages by artificial compensating algorithms. This factor is also responsible for the undesired diffracted orders. The pixelated structure yields a similar function but with a very high frequency, high enough to be neglected here.

Figure 2 illustrates a result from a holographic projection setup. The image design is shown in Figure 2(a), the desired image is shown in Figure 2(b), and the experimental result is shown in Figure 2(c) with a 532 nm continuous wave laser. The projection setup is much like the one shown before (Figure 1).

In Figure 2(a), the desired format is given such that the signal window is encircled by the dummy area to decrease noise and increase diffraction efficiency. Figure 2(b) demonstrates the mark scheme, which, essentially, is a cross shape. Figure 2(c) demonstrates the result, which can be mathematically formulated as in Equation (3). In the system, the CGH has a pixel size of $\delta = 2.4$ μm and a pixel depth of $\beta = 4$ nm. One unit element includes 64×64 pixels, for a total size of $L =$ 154 μm, replicated to cover the 1.5 mm diameter of the laser beam. Here, the device to screen distance is approximately f = 125 cm. The total size of the cross image is around 3 cm, which can also be computed numerically by the expression $\lambda f/\delta$ and by taking into account the proportion of the signal window to the total area. For the purpose of marking, one needs to get local intensity spots on the material. If these spots are too close, then the marking is not smooth; on the other hand, if they are too far, then the images will not be clear. From Figure 2(c), the separation of the spots is actually given by Equation (3), such that the comb function part equals the summation of $\delta(\xi - k(\lambda f/L))\ \delta(\eta - \ell(\lambda f/L))$. Briefly, Equation (3) can be interpreted as

$$Total\_image\_field(\xi,\eta) = \left[Desired\_image\_field(\xi,\eta)\sum_{k=-\frac{M}{2}}^{\frac{M}{2}-1}\sum_{\ell=-\frac{N}{2}}^{\frac{N}{2}-1}\left(\xi - k\frac{\lambda f}{L}\right)\left(\eta - \ell\frac{\lambda f}{L}\right)\right] \otimes \psi'(\xi,\eta) \quad (4)$$

where dummy variables k, ℓ are integers and ψ' is the Fourier transform of the modal field of the laser (the modal field is preserved under a transform, only changing the size). Equation (4) is for continuous coordinates; for discrete coordinates ξ, η can be exchanged with p, q, respectively. So, based on Equation (4), the separation caused by replication is $\lambda f/L$, which is 4.3 mm, and in good agreement with the experimental result. These energy spots facilitate fiducial mark formation, and each one carries the information of the incoming laser's modal pattern.

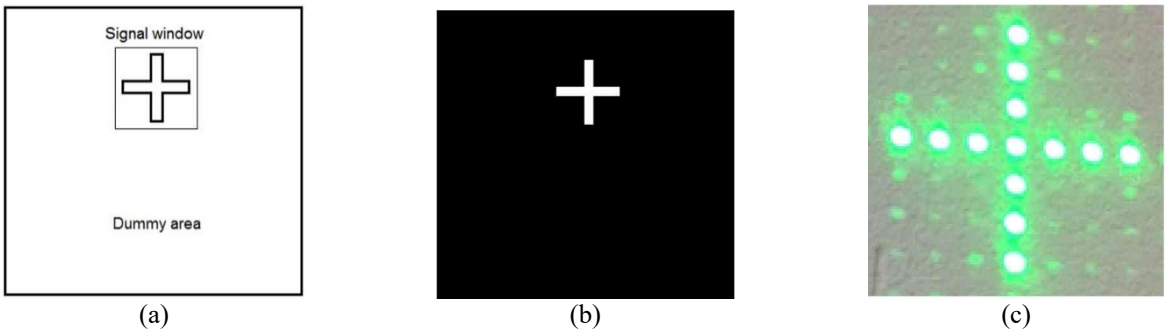

Figure 2. (a) Desired image format, including the signal window (not in proportion), **(b)** desired image intensity pattern, **(c)** final reconstructed image (main order). See text for more information.

3.2 Experiment

Now that the base CGH operation is demonstrated, it will be used to make marks on a silicon wafer. The silicon's laser damage threshold is relatively low. The experiment setup is illustrated in Figure 3. A pulsed laser, which is a frequency-doubled Nd:YAG, at 532 nm, delivering 4-10 mJ pulses having 7-10 ns pulse width, is collimated and projected through the CGH for beam shaping and eventual marking.

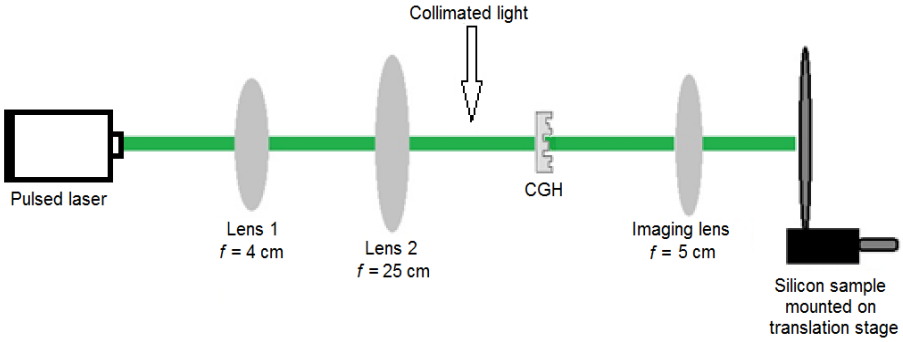

Figure 3. Fiducial marking setup, using silicon substrates. The first two lenses are for collimation, and the last lens is the imaging (Fourier) lens reconstructing at the focal plane.

3.3 Results

The results appear in Figure 4. The marking pattern is shown in Figure 4(a). In the scheme, the signal window is designed to encircle the critical area, where sensitive circuitry resides. Therefore, this area especially needs to stay clean in terms of light flux. Figure 4(b) is the image that is used in computing the element, and it shows the desired image that includes 4 crosses. Figure 4(c) is the image at the screen before the marking process. As shown, the dots are arranged so that they cover the entire image, and they do not coincide. This is done by adjusting the CGH parameters such as number of pixels and unit length. The distance between imaging lens and the screen equals the focal length of the lens, f = 5 cm. The parameters for the CGH are δ = 2.4 µm, β = 4 nm, and L = 1.2 mm. From those, the total image size is 11 mm, and each cross mark is 0.4 mm × 0.4 mm, as seen in Figure 4(d). For the experiment, one important figure is the size of the mark features, which is around 400 µm. By considering the highly multimodal laser, this feature size and the achieved image quality are quite remarkable. Note that in Figure 4(d), the black dot at the center was used for alignment purposes during

recording. In the image, the dotted pattern of each cross mark is seen; these individual local spots create the desired shape by creating the local intensity concentrations required to exceed the damage threshold of the material.

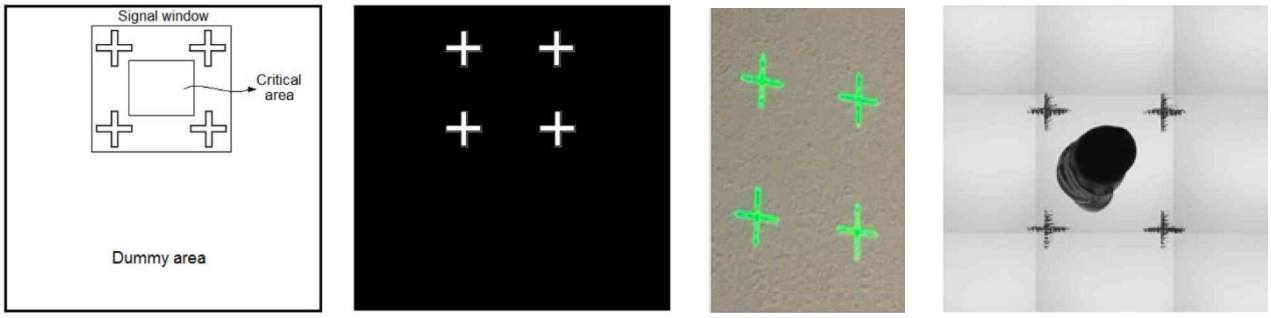

Figure 4. (a) Desired image format, including the signal window (not in proportion), **(b)** desired image intensity pattern, **(c)** final reconstructed image (main order), (d) final fiducial marks on a silicon substrate using the holographic projection technique. The size of each cross mark is 0.4 mm × 0.4 mm.

In designing the images, an off-axis configuration might be required as applied above. The reason for this is the undiffracted "zero-order" spot that generally occurs in diffractive elements. This central spot is caused mainly by fabrication errors and may damage the image quality. Although its effect can be lessened, it may not be totally removed. An off-axis design can shift the pattern and remove its effect completely.

4. CONCLUSION

4.1 CGH Fabrication

After explaining the main design and operational stages, it is beneficial to mention briefly the CGH fabrication details, since this element is the critical component for this study.

Fabrication of the CGHs consists of three main process steps: lithographic writing with photoresist, confocal microscopy to validate the design, and replication to plastic parts. Positive photoresist masters are exposed under a 405-nm laser controlled by a direct write lithography machine, by using a grayscale image file of the calculated hologram. Areas exposed with higher intensity or longer exposures will result in deeper features in the resist. These masters are developed and measured with a confocal microscope. The exposed areas are analyzed and compared to the targeted CGH structures. Errors are corrected by updating recording parameters, and a new master is exposed. This process is repeated until the difference between the target and exposed structures averages a root-mean-square (RMS) value of < 10 nm. Once the desired microstructure is fully developed, it is contact-transferred onto the surface of a silicone rubber master, which preserves the microstructure. This rubber master is then used to reproduce plastic parts, which are then used in the experiments. The parts used in this project consisted of a polycarbonate substrate carrying a special epoxy resin for embossed microstructures. Both materials have refractive indices around 1.52.

4.2 Summary

Making spots as small as possible has always been at the heart of optical engineering. In general, the spot diameter is directly related to wavelength, *f*-number of the imaging lens, and the laser beam divergence (M^2). Upon making fiducial marks, the experimenter is still bound by this limit such that the components (dots) constituting the marks cannot be smaller.

In this work, we executed fiducial marking on silicon substrates by using principles of holographic projection with a CGH that was specially designed for this purpose. We have achieved clear images of less than half a millimeter, with diffraction efficiency of 56%. In designing the CGHs, a number of pixels should be arranged to contain enough information. The size of the unit CGH element, L, can be estimated by taking the effects of spot separation into account, and the size of the entire diffractive structure, T, must guarantee coverage by the collimated laser beam. As trade-offs, a very small pixel size, δ, for example, will increase mark size in addition to more stringent requirements on fabrication. On the other hand, a very large pixel size will result in a large unit hologram size, yielding a low replication number, and this causes speckle noise on the

image. Therefore, all these parameters affect the result, and trade-offs must be handled carefully by also examining the governing equations and consequences, given mainly in Equation (3).

As mentioned before, the holographic projection method has obvious advantages over the classical approaches where one either uses an amplitude mask or dynamic laser deflection for etching. These approaches might have some disadvantages such as low efficiency, sensitive accuracy, or complicated machinery. In the holographic projection method with a CGH, which is actually a phase mask, one can get fast and accurate marking schemes that are also suitable for rapid prototyping.

4.3 Future Work

For analysis of semiconductor devices under a microscope, fiducial marks with sizes at micron ranges can be quite useful. To get smooth marks with the desired sizes, no matter which method is used, one needs to minimize the *f*-number of the system. By assuming that this is close to one, the laser needs to be optimized such that the wavelength will be small, radiating at the TEM_{00}. The laser of choice can be, for example, an argon fluoride excimer laser at 193 nm, which is commonly used in optical lithography applications[10], reducing the minimum feature size to 200 nm.

Therefore, upon using the right laser with a careful design, a micron size feature length of marks is possible with the holographic projection method. These marks will be compatible with the features of the circuitry and easily noticeable during inspection.

5. ACKNOWLEDGEMENTS

This work was supported by the U.S. Defense Microelectronics Activity (DMEA), contract number: HQ072718P0029. Any opinions, findings and conclusions or recommendations expressed in this material are those of the authors and do not necessarily reflect the views of the DMEA.

REFERENCES

[1] E. Buckley, "Holographic Laser Projection," Journal of Display Technology, 7(3), 135-140 (2011).
[2] M. Ekberg, M. Larsson, A. Bolle *et al.*, "Nd:YAG laser machining with multilevel resist kinoforms," Applied Optics, 30(25), 3604-3606 (1991).
[3] E. Neiss, M. Flury, and J. Fontaine, "Diffractive optical elements for laser marking applications," SPIE Photonics Europe. 7003, 70032L.
[4] D. Gabor, "A New Microscopic Principle," Nature, 161(4098), 777-778 (1948).
[5] G. Tricoles, "Computer generated holograms: an historical review," Applied Optics, 26(20), 4351-4360 (1987).
[6] B. R. Brown, and A. W. Lohmann, "Computer-generated Binary Holograms," IBM Journal of Research and Development, 13(2), 160-168 (1969).
[7] D. Voelz, [Computational Fourier optics: a MATLAB® tutorial] SPIE, Bellingham, Washington (2011).
[8] D. W. Prather, A. D. Kathman, T. J. Suleski *et al.*, [Diffractive Optics: Design, Fabrication, and Test] SPIE, Bellingham, Washington (2003).
[9] J. W. Goodman, [Introduction to Fourier optics] Roberts & Co., Greenwood Village, Colorado (2005).
[10] J. Hecht, [Understanding lasers: an entry-level guide] Wiley-IEEE Press (2019).